Rheology of aqueous foams

Benjamin Dollet, Christophe Raufaste

Rheology of aqueous foams

Benjamin Dollet*

Institut de Physique de Rennes, UMR CNRS 6251,

Université de Rennes 1, Campus de Beaulieu, 35042 Rennes Cedex, France

Christophe Raufaste†

Université Nice Sophia Antipolis, CNRS,

LPMC, UMR 7336, 06100 Nice, France

(Dated: August 27, 2014)

Abstract

Aqueous foams are suspensions of bubbles inside aqueous phases. Their multiphasic composition leads to a complex rheological behavior that is useful in numerous applications, from oil recovery to food/cosmetic processing. Their structure is very similar to the one of emulsions so that both materials share common mechanical properties. Meanwhile the gas-liquid interfaces and the presence of surfactants lead to peculiar interfacial and dissipative properties. Foam rheology has been an active research topics and is already reported in numerous reviews. Most of them cover rheometry measurements at the scale of the foam, coupled with interpretations at the local - bubble or gas-liquid interface - scale. In this review we first start following this approach, then we try to cover the multiscale features of aqueous foam flows, meaning that we emphasize here regimes where intermediate length scales need to be accounted for or regimes fast enough regarding internal time scales so that the flow goes beyond the quasistatic limit.

PACS numbers: 83.80.Iz Emulsions and foams

* benjamin.dollet@univ-rennes1.fr

† christophe.raufaste@unice.fr

I. INTRODUCTION

Liquid foams are comprised of gas bubbles separated by a liquid continuous phase. The latter is generally an aqueous solution of amphiphilic molecules called surfactants, which stabilise the liquid films between bubbles. Foams are characterised by structural and geometric parameters, like the average bubble size and the polydispersity and, most importantly, the liquid fraction ϕ_ℓ. In opposition to bubbly liquids, foams are usually classified as those bubble suspensions which are below a critical liquid fraction ϕ_ℓ^c, given by the random close packing fraction for a disordered foam (36% in 3D [73]). Its packing is characterized by the distance to the rigidity loss transition $\Delta\phi_\ell = \phi_\ell^c - \phi_\ell$, where $\Delta\phi_\ell = 0$ corresponds to the loss of rigidity of the foam and a transition to a dilute gas-bubble suspension. The transition from a dilute gas-bubble suspension to a foam, called jamming transition, occurs for the same value ϕ_ℓ^c so that we will use both terms in what follows [73].

The properties of foams are intimately related to their structure, which we briefly describe in the static case; see e.g. Cantat et al. [16], Weaire and Hutzler [142] for extensive discussion. At low liquid fraction, bubbles are bounded by thin films, of thickness lower than 1 μm. Such films meet threefold along lines, the so-called Plateau borders (Fig. 1a). Plateau borders meet fourfold at vertices (or nodes) (Fig. 1b). At equilibrium, the geometry of this structure obeys the so-called Plateau rules [112] that films meet at 120°, and Plateau borders at the tetrahedral angle $\arccos(-1/3) \simeq 109.5°$. At finite liquid fraction, liquid covers this "skeleton" of vertices and Plateau borders. The cross section of the Plateau borders occupied by the liquid forms a concave triangle, of constant radius R, hence of area $(\sqrt{3} - \pi/2)R^2$. The volume of liquid at a vertex is of order R^3. For not too wet a 3D foam, most of the liquid is in the Plateau borders, whence a scaling relation between the liquid fraction ϕ_ℓ, the typical size of the bubbles a, and the radius R: $\phi_\ell \approx R^2/a^2$. When bubbles are bounded by a flat wall, such is the case of 2D foams made of a bubble monolayer (Fig. 2), the films meet the wall at right angle. For an ideal 2D foam, there is an exact relation; since there are in average six threefold vertices around a bubble, we have: $\phi_\ell = (2\sqrt{3} - \pi)R^2/A$, with A the average area per bubble [118].

Because of their multiscale structure, liquid foams display a complex mechanical behaviour: they have elastic, plastic and viscous properties. This qualifies foams as complex fluids, like colloidal and granular suspensions, polymers, pastes, slurries and emulsions [25],

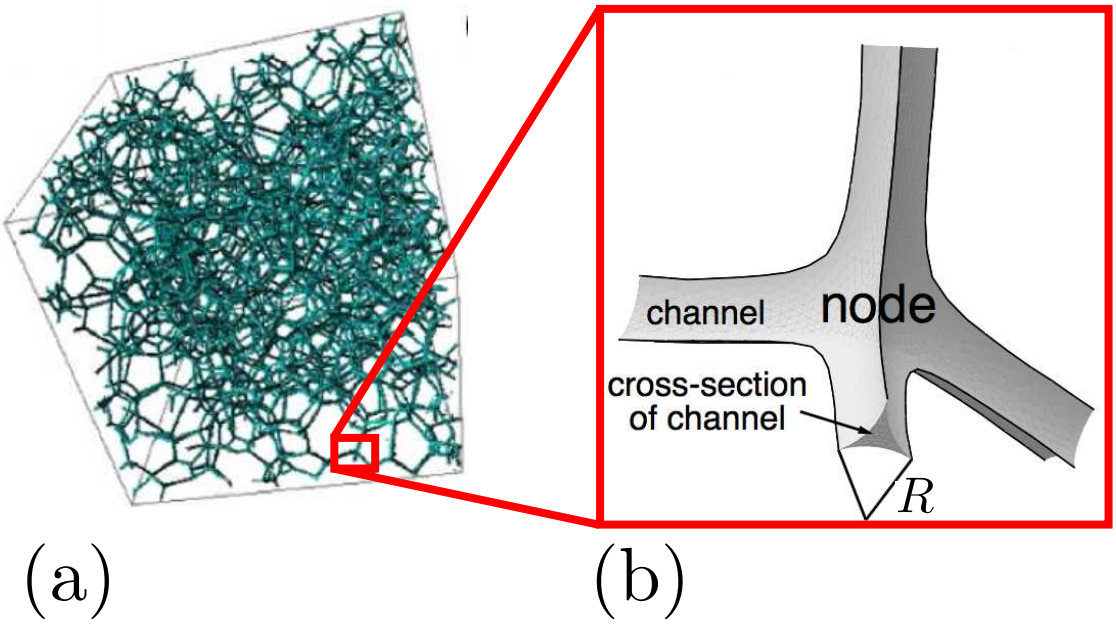

FIG. 1. (a) Reconstruction of the Plateau border network inside a 3D dry foam by X-ray tomography (from Lambert et al. [85]). (b) A vertex or node is defined as the fourfold junction between four Plateau borders (image adapted from Koehler et al. [77]).

and the measurement and understanding of their complex mechanical response belongs to the field of rheology [87, 92].

Foams share many common properties with emulsions, which are dispersions of liquid droplets in another liquid phase. In particular, they are ruled by the same structural properties, and they are athermal systems in the sense that their microstructural items (the bubbles or the droplets) are too big to feel thermal fluctuations, in contrast with other complex fluids like polymers or colloidal suspensions. As a natural consequence, foams and emulsions have a very similar rheological behaviour, and we shall henceforth mention several examples from experimental studies on emulsions.

Foam rheology has been an active research topics for at least the past thirty years, and there exists already many good reviews of this topic [23, 35, 62, 73, 78], which is also covered in various book chapters [16, 134, 142]. Most of these reviews report experiments based on rheometry, giving macroscopic measurements at the level of the foam as a whole, and their interpretation at the local scale. Here, although we start following a similar path, we devote a large part on local measurements, especially velocity fields. On the other hand, we have

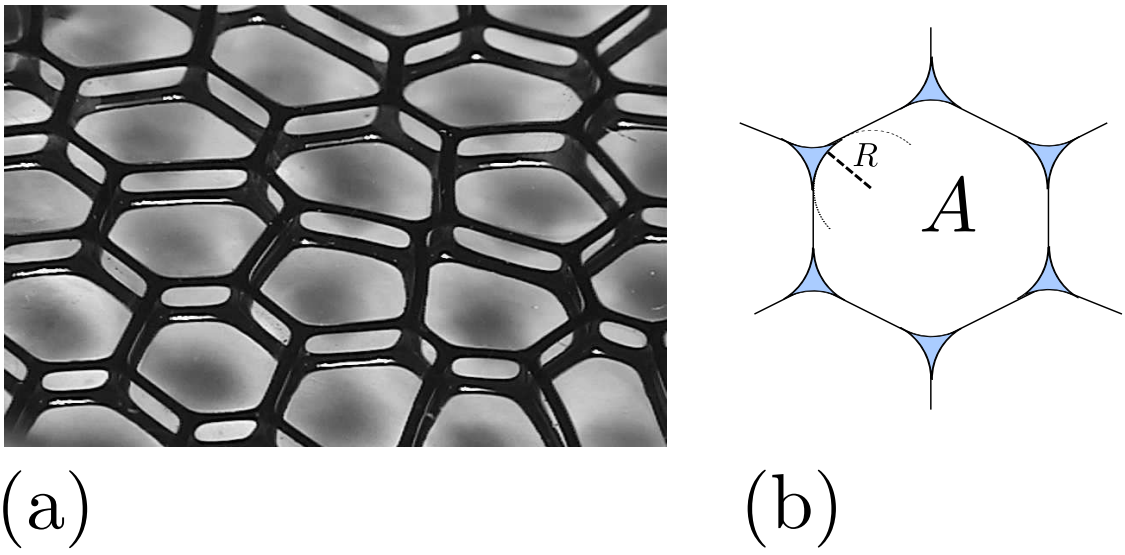

FIG. 2. 2D foam. (a) Monolayer of a ferrofluid foam between two glass plates. Image courtesy of Eric Janiaud. (b) Bubble inside an ideal 2D foam. The Plateau border cross-section is formed of three arcs of a circle of radius R that meet tangentially along the bubble faces [118].

chosen not to cover interesting subjects as the rheology of highly confined foams, found in porous media (see e.g. [65, 122]) and microfluidics (see [97] for a review), when the foam is reduced to organised structures or separated lamellae. We also focus on aqueous foams, although the rheology of non-aqueous foams [128] and of Langmuir foams [24, 37], formed at interfaces populated by insoluble surfactants in conditions of phase coexistence, would certainly deserve a discussion.

Our manuscript is organised as follows. In Sec. II, we review rheometric measurements on liquid foams, which have evidenced their viscoelastic and viscoplastic behaviours. In Sec. III, we report the models that have aimed at explaining the origin of such an intricate mechanical behaviour, from micromechanical models of elasticity, yield and dissipation to more generic approaches. In Sec. IV, we show that when the foam is confined, the connection between a local scale (typically that of a single bubble) and the global foam flow is not direct and other scales come into play, either because of the friction against a confining wall or because of the finite range of influence of individual plastic events. Finally in Sec. V, we present the peculiar behaviour of foams as they depart from their equilibrium structure, when they are subjected to high shear rates or high frequencies.

II. RHEOMETRY OF FOAMS

A most classical way to probe the mechanical properties of foams is rheometry, where foams are sheared at rate $\dot{\gamma}$ by a rheometer in various geometries: between two planes, or a cone and a plane, or two cylinders (the so-called Couette rheometer), at a shear stress τ as constant as possible [87, 92]. A classical experiment in rheometry consists in subjecting the foam to an oscillatory shear of angular frequency ω: $\gamma = \gamma_0 \cos \omega t$, of small strain amplitude $\gamma_0 \ll 1$. Measuring a harmonic stress response: $\tau = \gamma_0[G'(\omega) \cos \omega t + G''(\omega) \sin \omega t]$ gives the elastic modulus G' and the loss modulus G'': this is a linear viscoelastic characterisation of the foam. Plotting the elastic and loss moduli as functions of the frequency, three regimes are usually observed (Fig. 3). At intermediate frequency, G' and G'' display roughly plateaus, and G'' is usually one order of magnitude smaller than G'. Hence, foams respond mostly elastically, but with a significant dissipation accompanying the deformation. As low frequency, both G' and G'' decrease, and G'' overtakes G'. This is a signature of the influence of coarsening on foam rheology [22, 99]. At high frequency, G' and G'' increases with a nontrivial power law of exponent 1/2 [58, 82, 91, 100].

At a frequency such that G' and G'' are in the plateau regime, several groups have investigated the effect of the strain amplitude [99, 100, 124–126] (Fig. 3). Below a critical strain γ_c which decreases with the liquid fraction, the elastic and loss modulus are roughly constant: this is a linear regime. Above γ_c, G' is a decreasing function of the strain amplitude, whereas G'' usually shows a maximum and overtakes G', before decreasing with the strain amplitude. Hence the critical strain γ_c is identified as a yield strain, above which the foam start to flow.

To investigate flow regimes, many authors have measured the stress response of foams subjected to a constant shear rate $\dot{\gamma}$ (Fig. 4). The measurements are usually well fitted by the Herschel–Bulkley law:

$$\tau = \tau_y + A\dot{\gamma}^n, \tag{1}$$

with a finite yield stress at vanishing shear rate which decreases with liquid fraction, and a sublinear increase (notice that $n = 1$ would correspond to the so-called Bingham model). Experiments show generally an exponent close to 0.5 [35, 98, 108, 109, 116, 137] or lower [35, 109, 137]

Rigidity of the foam is probed by measuring quantities such as G' and τ_y as functions

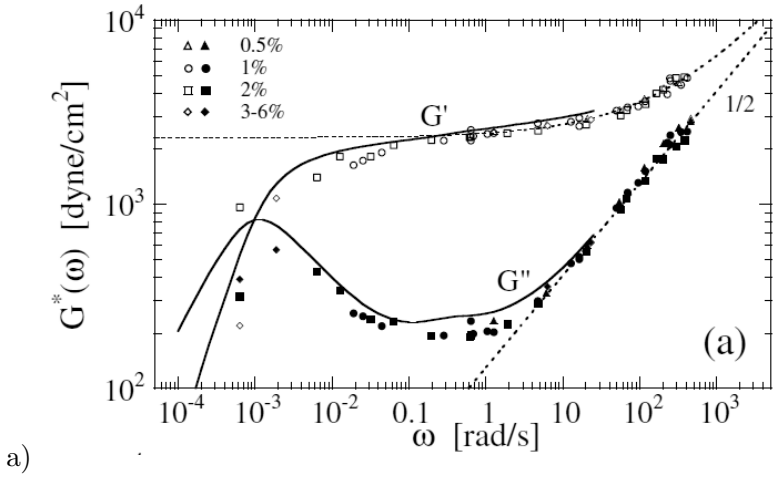

a)

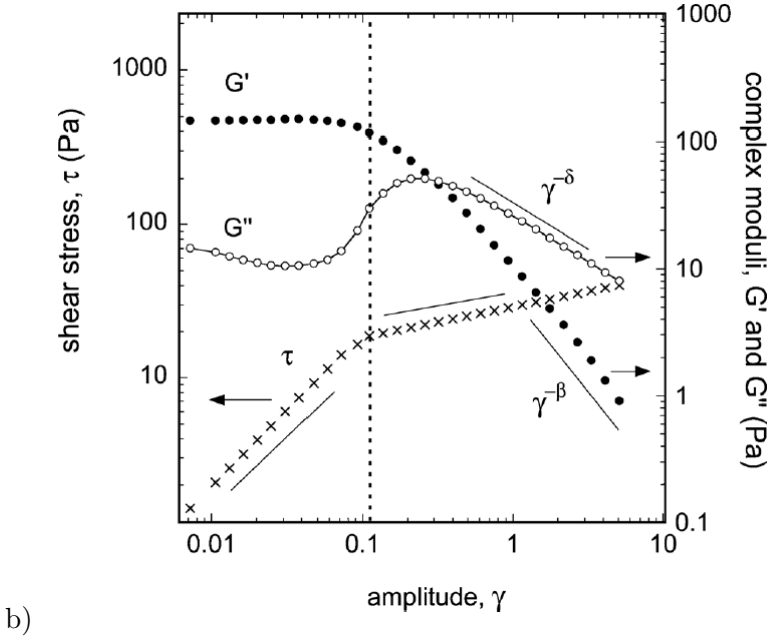

b)

FIG. 3. Oscillatory rheometry. a) Elastic modulus G' (open symbols) and loss modulus G'' (filled symbols) as a function of the angular frequency. The sample is a Gillette foam, of bubble size 60 μm and liquid fraction 8%. The different symbols stand for different values of the shear amplitude γ_0. From Gopal and Durian [58]. b) Elastic modulus G' (open symbols) and loss modulus G'' (filled symbols) as a function of the strain amplitude. The sample is a SDS foam, slightly polydisperse, of mean bubble radius 60 ± 5 μm and liquid fraction 15%. From Marze et al. [99].

of the liquid fraction ϕ_ℓ [99, 126]. Such quantities vanish as the liquid fraction reaches the critical liquid fraction of the rigidity loss transition (Fig 5).

These rheometric studies show that below a yield strain or a yield stress, foams behave as viscoelastic solids, while they flow as non-Newtonian liquids above yield.

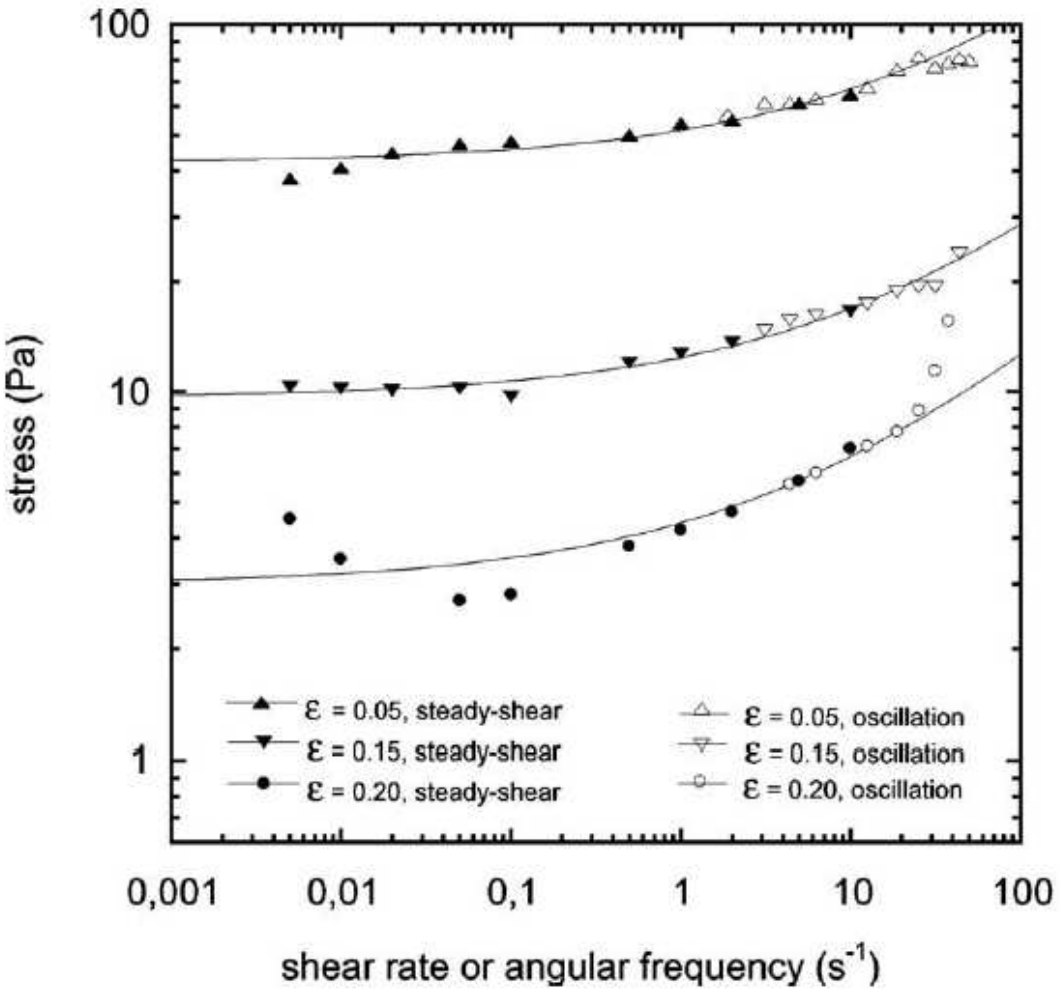

FIG. 4. Constant shear rate rheometry. Stress as a function of the shear rate. The samples are SDS foams, at various liquid fractions (denoted, here only, ε). From Marze et al. [98].

If edge bubbles of the foam sample are not fixed to the rheometer walls all inside the apparatus, for instance by roughening the rheometer walls with sandpaper, there is a certain amount of wall slip that has to be corrected to correctly interpret the measurements [98, 116]. If slip occurs, as for foams confined by smooth walls, there is an extra frictional stress depending on the slip velocity.

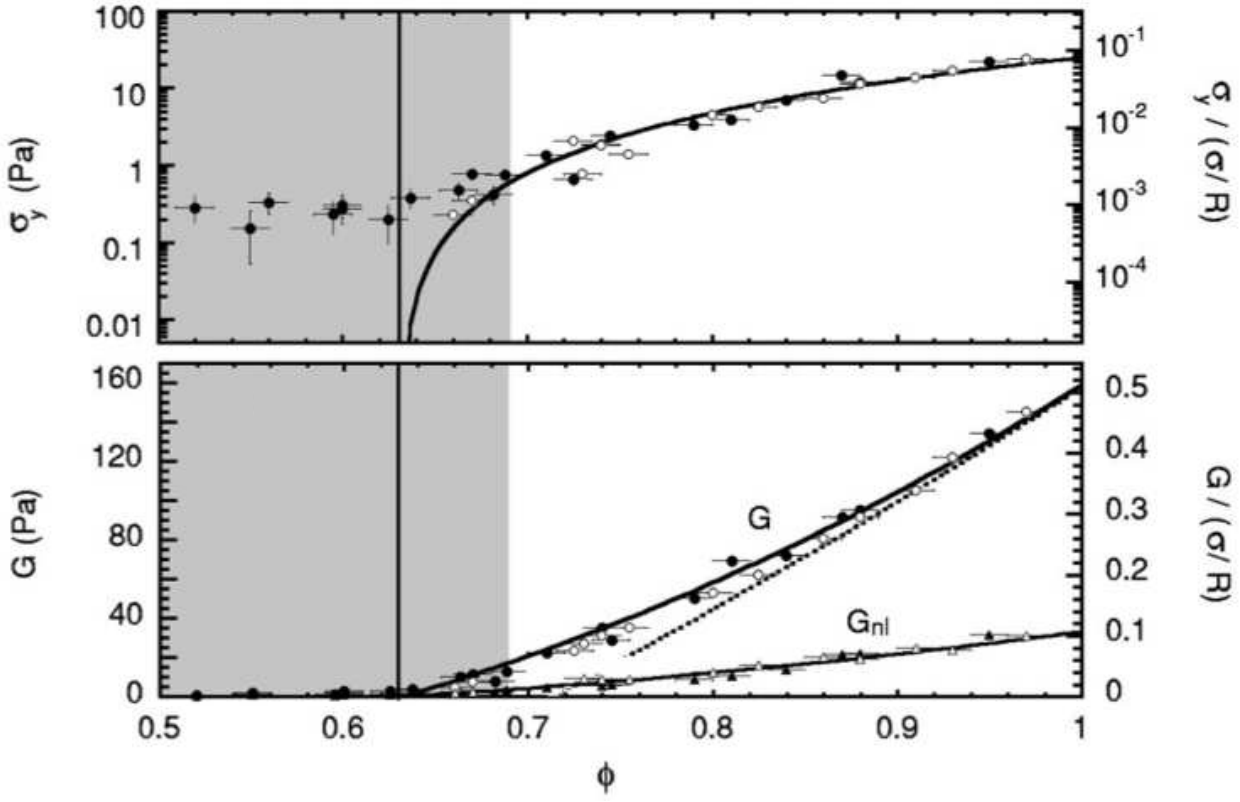

FIG. 5. Adapted from [126]. Top: The yield stress τ_y (here σ_y) or its dimensionless value $\tau_y/(\sigma/a)$ (here $\sigma_y/(\sigma/R)$) as a function of the packing fraction $\phi = 1 - \phi_\ell$. The solid line, proportional to $\Delta\phi_\ell^2$, represents the empirical results found for monodisperse emulsions [101]. Bottom: The shear modulus G' (here G, circles) or its dimensionless value $G'/(\sigma/a)$ (here $G/(\sigma/R)$) as a function of the packing fraction $\phi = 1-\phi_\ell$. The continuous lines represent the Mason's formula, $\propto (1-\phi_\ell)\Delta\phi_\ell$ [100], while the dashed line is Princen's formula, $\propto (1-\phi_\ell)^{1/3}\Delta\phi_\ell$ [115].

III. LOCAL ORIGINS AND MODELLING OF FOAM RHEOLOGY

A. Visualisation of elasticity and plasticity

The local manifestations of elasticity and plasticity are easy to visualise in 2D foams (Fig. 6). At equilibrium, bubbles are in average undeformed; they appear as polygons (or polyhedra in 3D), with more or less rounded vertices depending on the liquid fraction (Fig. 6a). Under forcing, they can deform (Fig. 6b). The total area of their bounding interface, hence their surface energy, then increases: they store some elastic energy, proportional to the surface tension. Above a certain level of deformation, they undergo topological re-

arrangements, the so-called T1 events. An elementary T1 involves always four bubbles in 2D, and in most cases in 3D [7, 120, 121]. During such an event, two bubbles lose contact, whereas two of their neighbours come into contact (Fig. 6c, d and e). This process leads to a saturation of the stored elastic energy, hence to the existence of a yield stress.

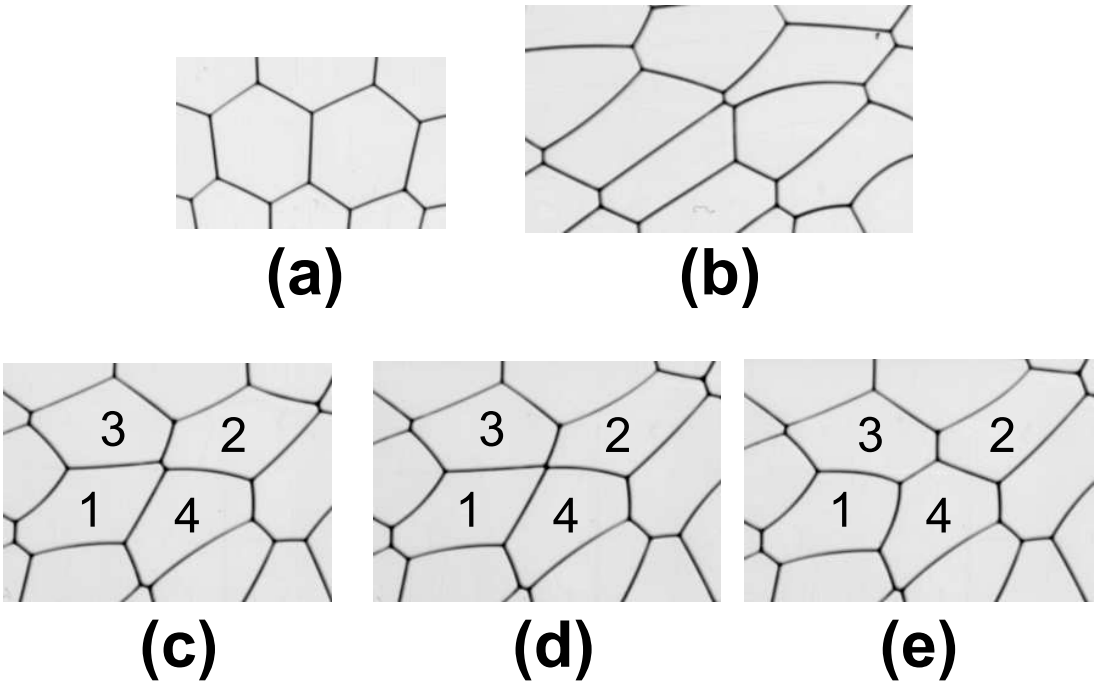

FIG. 6. (a) Snapshot of undeformed bubbles in a dry 2D foam (liquid fraction 0.3%). (b) Deformed bubbles, storing elastic energy. Illustration of a plastic rearrangement T1, whereby bubbles labelled 1 and 2 lose contact whereas 3 and 4 come into contact; (c) before the T1, (d) at the instant of the T1, with a transient fourfold vertex; (e) after the T1.

B. Models of elasticity and yield

The elastic properties of foams are linked to the variation of their total interfacial area. Batchelor [3] showed that the elastic stress calculated over a representative volume element of volume V equals: $\tau_{ij}^{\mathrm{el}} = \frac{\sigma}{V}\int(\delta_{ij} - n_i n_j)\mathrm{d}S$, where the integral is computed over all the gas/liquid interfaces comprised inside V. Hence for a monodisperse foam with a the radius of the undeformed bubbles, the elastic modulus and yield stress scales as σ/a; as an order of magnitude, for $\sigma \approx 3 \times 10^{-2}$ N/m and $a \approx 10^{-4}$ m, this gives $G' \approx 3 \times 10^{2}$ Pa. This is

much lower than the bulk modulus of foams which, since foams are constituted mostly of gas, is of the same order of magnitude as the ambient pressure, 10^5 Pa. As a consequence, foams can be considered as incompressible in most cases.

To predict the exact value of the shear modulus and yield stress, and their dependence on liquid fraction, several authors starting from Princen [113] have considered the quasistatic deformation of the perfectly ordered and monodisperse 2D hexagonal foam, invariant along the third direction. If the liquid fraction is zero, the foam is a honeycomb lattice (Fig. 7). It is subjected to an external strain (simple shear, or elongation), and the midpoints of all edges are assumed to follow the applied strain. The position of the vertices then follows from the Plateau rule: three edges meet at equal angles of 120°. This enables to compute the structure at any strain step (Fig. 7), hence the elastic stress as a function of strain. In particular, this gives the shear modulus as $G' = \mathrm{d}\tau_{xy}/\mathrm{d}\gamma|_{\gamma=0}$. The calculations show that $G' = \sigma\sqrt{3}/6a$, whatever the relative orientation of the lattice and the shear [75]. Here (and only here) a stands for the side length of a regular hexagon.

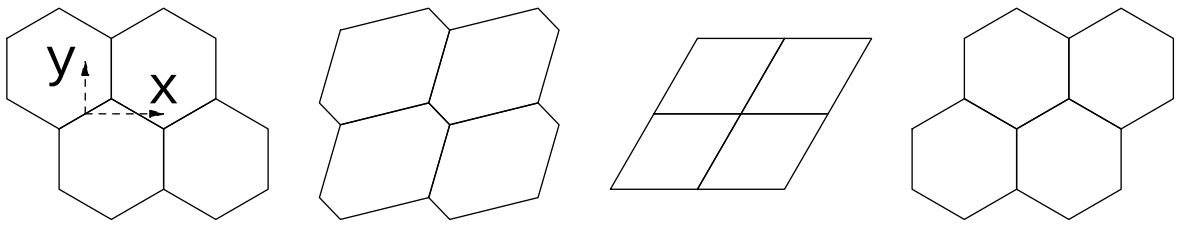

FIG. 7. Evolution of a honeycomb lattice subjected to a simple shear γ (here, aligned with the x direction). From left to right, $\gamma = 0$; $1/\sqrt{3}$; $2/\sqrt{3}$, where the T1 occurs; and relaxed state after the T1.

Moreover, the calculation gives the yield strain, as the strain at the moment where the shortest of the bubble edges shrinks to zero. In the particular case where the lattice and the shear are aligned (Fig. 7), it equals $2/\sqrt{3}$, but contrary to the shear modulus, it depends on orientation [75]. From the structure at the yield strain, the yield stress can also be deduced; in the present case, it equals $\tau_y = \sigma/a\sqrt{3}$, and it also depends on orientation [75]. At the yield strain, a topological rearrangement T1 occurs: the transient fourfold vertex is unstable, and the foam spontaneously relaxes towards a new equilibrium configuration. During this relaxation, which is not described by the quasistatic model, some energy is dissipated, because the total surface energy decreases. The modes of dissipation then set

the duration of the relaxation phase after a T1 [7, 46, 53, 90]. The order of magnitude of dissipated energy per T1 is thus σa.

At finite liquid fraction, the calculation is modified by the presence of the concave triangles at the vertices (Sec. I) [76, 113]. This barely affects the shear modulus, but strongly reduces the yield strain and the yield stress, which vanish for $\phi_\ell = 1 - \pi/2\sqrt{3} \simeq 9.3\%$ in the case of the perfectly ordered and monodisperse 2D hexagonal foam.

In the same spirit, in 3D, Reinelt and Kraynik [120], Kraynik and Reinelt [80] and Reinelt and Kraynik [121] have studied numerically the simple shear of ordered 3D foam structures, notably the Kelvin foam. The qualitative conclusions remain the same, with the extra feature that the shear modulus is anisotropic.

To model the influence of disorder on the elastic properties of foams, Derjaguin [38] considered in a pioneering paper that the foam is an assembly of randomly oriented films, which are sheared affinely. The shortcoming of such an approach is that it ignores the Plateau rules, and it overestimates the shear modulus. Stamenović [133] considered a foam constituted of an assembly of tetrahedra, satisfying to the Plateau rules, and derived a more realistic shear modulus.

Area and edge length, polydispersity have also been considered as "perturbations" of the ordered case [83] and measurements of shear modulus have been related to disorder in simulations [27], but both studies are performed in 2D. The only simulations of 3D polydisperse foam [81] reveal the role of the surface-volume mean bubble radius to account for the effect of polydispersity. It remains a challenge to account for disorder yet retaining Plateau rules, and promising descriptions began to appear only recently [47, 103].

The influence of the liquid fraction ϕ_ℓ on the packing rigidity was first probed on emulsions [84, 100–102, 114, 115]. Regarding the yield stress, Princen suggested an extension in 3D [114] of its 2D geometrical model [113], leading to $\tau_y \propto \sigma/a \times \phi_\ell^{1/3} \tilde{F}_{max}(\Delta\phi_\ell)$, where $\tilde{F}_{max}$ is the dimensionless contribution per drop to the yield stress and is expected to vary from 0 at the jamming transition, $\Delta\phi_\ell = 0$, to a maximal value for $\phi_\ell = 0$. Both Princen [114] and Mason et al. [101] found empirically that $\tilde{F}_{max} \sim \Delta\phi_\ell^2$ for their emulsions. Under the same geometrical considerations, Princen and Kiss [115] deduced an expression of the shear modulus G' versus the liquid fraction as $G' \propto \sigma/a \times (1-\phi_\ell)^{1/3}\Delta\phi_\ell$. Lacasse et al. [84] suggested a model based on individual interactions between droplets. On the assumption of an anharmonic potential between droplets in contact, they found $G' \propto \sigma/a \times (1-\phi_\ell)\Delta\phi_\ell$ which

was in better agreement with their experiments on emulsions, but also with experiments on foams performed latter on [126] (Fig. 5).

C. Origins of dissipation

1. *Bulk dissipation*

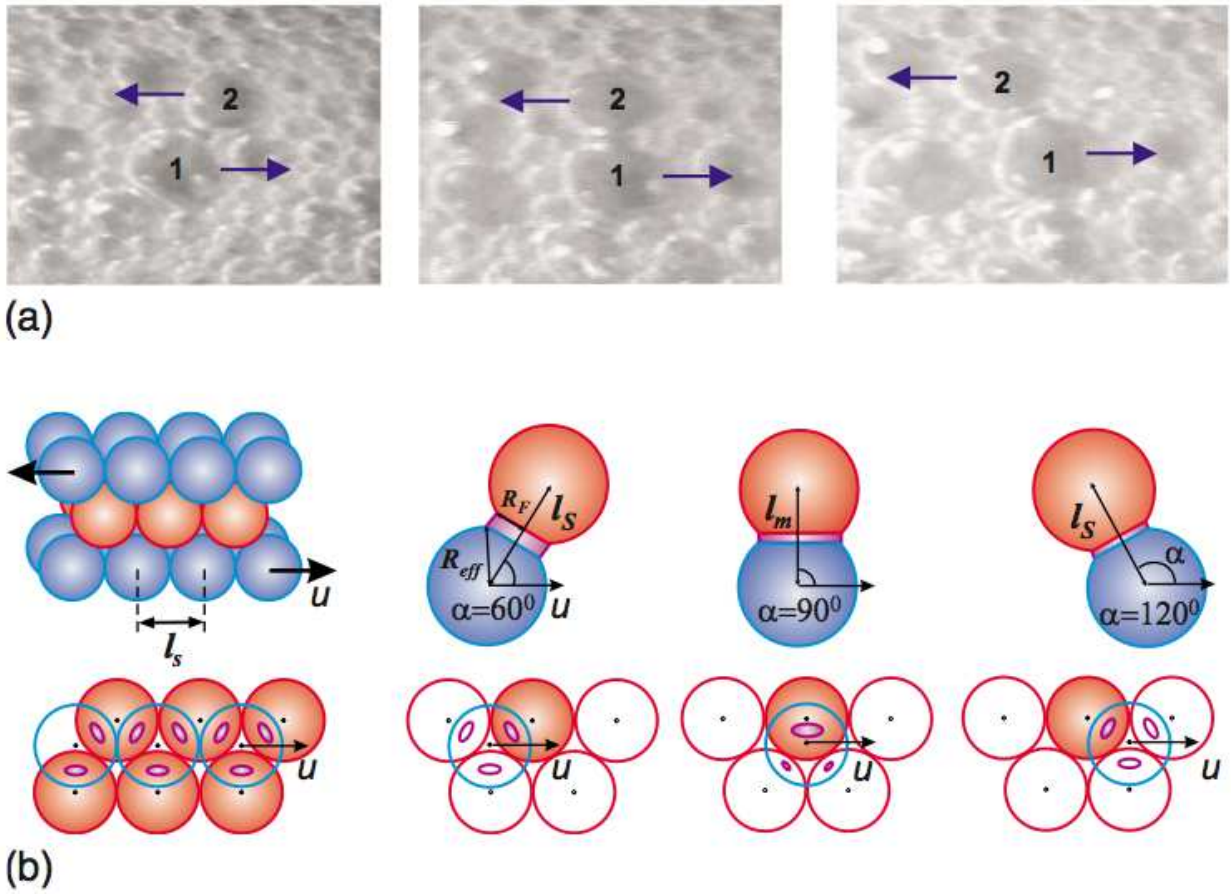

FIG. 8. Bubble friction inside a liquid foam, from Tcholakova et al. [137]. (a) Images of the process of bubble friction of bubbles passing along each other in sheared foam. (b) Schematic representation of the relative motion of planes of bubbles sliding along each other and of the process of film formation and disappearance between two bubbles.

Contrary to elasticity, there is no clear consensus about the origin of dissipation in foams, owing to the complex dynamics of surfactants [86], which can lead to many different modes of dissipation [13]. Here, we discuss only two limiting boundary conditions at the gas/liquid

interfaces: free shear, and no-slip.

Let us examine first the simplest free shear case, where the origin of dissipation is yet quite subtle [119, 129]. It is related to the gradient of capillary pressure between the curved Plateau borders and the flat films. At equilibrium, this capillary suction from the Plateau borders is balanced by the disjoining pressure, arising from repulsive interactions between the two interfaces bounding the films (see e.g. [63, 135]), which sets the thickness of soap films at rest of a few tens of nanometers. When the foam flows, the situation changes and the capillary suction is balanced by hydrodynamic forces. Assuming a relative velocity U between a film of thickness h and a Plateau border or radius R, the flow is driven by the capillary pressure gradient over a transition zone of extent ℓ: $\sigma/R\ell$, which balances the viscous term: $\eta U/h^2$, assuming $h \ll \ell$, and with η the viscosity of the solution. Together with the scaling of the curvature of the transition region: $1/R \approx h/\ell^2$, this imposes the following scalings: $\ell \approx R\mathrm{Ca}^{1/3}$ and $h \approx R\mathrm{Ca}^{2/3}$, with $\mathrm{Ca} = \eta U/\sigma$ the capillary number. The dissipated power per unit length is thus of order $\eta(U/h)^2 h\ell \approx \eta U^2/\mathrm{Ca}^{1/3}$. Hence, the dissipated power per unit volume of foam is $\eta U^2/\mathrm{Ca}^{1/3}/a^2 \approx \eta(\sigma/\eta\dot\gamma a)^{1/3}\dot\gamma^2$, since $U \approx \dot\gamma a$. Hence, in the frame of this approach, the viscous stress scales as $\tau_v(\dot\gamma) \approx (\sigma/a)^{1/3}(\eta\dot\gamma)^{2/3}$.

In the opposite case of no-slip boundary condition, bubbles entrain their surrounding interfaces at their own velocity. This gives rise to a strong shear inside the appearing/disappearing films between bubbles sliding past each other (Fig 8). This case was treated in [34, 137], who proposed a different scaling: $\tau_v(\dot\gamma) \approx \sigma\mathrm{Ca}^{0.465}(1-\phi_\ell)^{5/6}/a\phi_\ell^{0.5}$, in good agreement with their experiments and where the small deviation from the exponents 1/2 regarding Ca is due to a geometrical factor. Considering both the foam films and the meniscus region, the authors derive a semiempirical formula for rigid interfaces considering the total viscous stress as a superposition of the friction in both regions [137]

$$\tau_v(\dot\gamma) \simeq \frac{\sigma}{a}\left[0.7\mathrm{Ca}^{0.47}\frac{(1-\phi_\ell)^{5/6}}{\phi_\ell^{0.5}} + 8\mathrm{Ca}^{0.7}\frac{(1-\phi_\ell)^{5/6}}{\phi_\ell^{0.15}}\right],$$

Experimentally, this formula works quite well for emulsions. For foams, dissipation inside the meniscus region seems overestimated and effect of the foam films is always dominant. The authors suggest that the no-slip boundary condition does not hold in the meniscus region, which decreases locally the shear [137].

Both these predictions of the viscous stress are sublinear in shear rate, in qualitative agreement with the experiments. This comes from the fact that the film thickness, over which

the liquid is sheared and dissipates energy, is determined by a balance between capillarity and hydrodynamics, and thus increases with its velocity relative to the reservoir from which it is extracted. This result is known as Frankel's law [107] for films withdrawn from a pool of solution, and it has been shown to apply also between a film and a Plateau border, either indirectly [8] or directly [130].

As mentioned in Sec. II, most experiments report exponents of order 1/2, or lower, for the dependence of the viscous stress on shear rate. As already pinpointed by Princen and Kiss [116], this seems to rule out the assumption of free shear boundary condition at the gas/liquid interface, which leads to an exponent 2/3, and to favour the assumption of rigid condition. However, the crossover criterion between two such extremes remains an open issue, and motivates currently active research in the context of soap film formation [127, 131]. Moreover, neither of the two limiting cases of free shear and no-slip boundary conditions explains the existence of exponents lower than 0.5. Since such exponents were observed with surfactants having high surface elasticity and viscosity, Tcholakova et al. [137] argued that they could be associated to surface dissipation within the gas/liquid interfaces; however, they did not provide explicit predictions for the exponent.

2. Foam–wall friction

Foam–wall friction is the main source of dissipation in confined foams. It is closely related to dip coating [145], and to the motion of isolated bubbles in tubes [11]. Like for foam bulk dissipation, two limiting cases have been treated: free shear and no-slip boundary conditions. For free shear boundary conditions, the arguments presented in Sec. III C 1 apply and the resulting prediction for the shear stress at the wall is [32]: $\tau_w \approx \sigma \mathrm{Ca}_w^{2/3}/a$, with a capillary number based on the sliding velocity U_w: $\mathrm{Ca}_w = \eta U_w/\sigma$. The no-slip case was treated by Denkov et al. [33] who showed that $\tau_w \approx \sigma \mathrm{Ca}_w^{1/2}/a$, although Cantat [15] proposed a correction for the 1/2 exponent. These expressions of the wall shear stress have been found to be in good agreement with experiments [32, 33]. However, here also, the crossover between the two extreme regimes remains to be quantified and explained.

D. Other approaches

Instead of building a model from realistic local details of the foams, several approaches have attempted to predict from generic ingredients the rheological behaviour of foams, and more generally of complex fluids, like the existence of a yield stress, or the scaling of the viscous stress.

A popular approach is the Soft Glassy Rheology model [132], inspired from glass models. It describes the evolution of a system described by an internal strain ℓ_i and a shear modulus k, and a distribution of elastic energy at yield, E. As an external shear is applied, the system can either elastically increase its strain, or plastically relax it, at a rate $\exp[-(E-k\ell_i^2/2)/x]$, with x an effective temperature related to the mechanical noise within the system. This theory captures many rheological behaviours: Newtonian fluids, power-law fluids, or yield stress fluids, depending on the value of the mechanical noise. However, it does not describe the full dynamics of relaxation in foams [22, 58]. Another popular approach is the Shear Transformation Zone theory [52]. It described the evolution of the population of plastic sites (the so-called shear transformation zones) in a sheared material. These zones have two possible states: fluid and jammed. They are created, annihilated, and they undergo transitions between the two states, at rates depending on the stress and strain rate. Like the SGR theory, this model captures many rheological behaviours.

More recently, models of complex fluids have been proposed by focussing on the distance to the jamming transition [73]. In the spirit of the so-called bubble model [48], Tighe et al. [139] assumed that neighbouring bubbles i and j of radii $R_{i,j}$, positions $\vec{r}_{i,j}$ and velocities $\vec{v}_{i,j}$ interact with an elastic force $f_{\rm el} \sim \delta^{\alpha_{\rm el}}$ if they overlap by an amount $\delta = R_i+R_j-|\vec{r}_i-\vec{r}_j| > 0$, and with a sliding friction force $f_{\rm visc} \sim |\Delta\vec{v}|^{\alpha_{\rm visc}}$ with $\Delta\vec{v} = \vec{v}_i - \vec{v}_j$, where α_{el} and α_{visc} stand for the exponent of the elastic and viscous interactions. The system subjected to a shear rate $\dot\gamma$ receives a power $\sigma\dot\gamma$, which is dissipated by friction, hence the power balance $\sigma\dot\gamma \sim f_{\rm visc}|\Delta\vec{v}|$. A relation $\sigma = g\gamma_{\rm eff}$ is then postulated between the stress and an effective strain $\gamma_{\rm eff} \sim \Delta\phi_\ell + a\dot\gamma/|\Delta\vec{v}|$, with two contributions: a yield strain assumed to be of the order of the distance to the jamming transition $\Delta\phi_\ell$, and a dynamic strain which is the typical strain between plastic events, the time between two consecutive such events being of order $a/|\Delta\vec{v}|$. The shear modulus g is assumed to scale with $\Delta\phi_\ell$ and $\gamma_{\rm eff}$, considering the jamming transition as a critical point [140, 148]: $g = \sigma/a \times \sqrt{\Delta\phi_\ell} \times \tilde{g}(\gamma_{\rm eff}/\sqrt{\Delta\phi_\ell})$, with

a dimensionless function $\tilde{g}$ having a finite limit at 0 and $\tilde{g}(x) \underset{x\to+\infty}{\sim} x$; recently, Jorjadze et al. [67] has confirmed this leading order, but with significant corrections, from a precise visualisation using confocal microscopy of the contacts in an emulsion. Tighe et al. [139] predict four rheological regimes (yield stress, transition, critical and viscous) with different scalings of the stress on both shear rate and distance to jamming. A particularly interesting outcome of this approach is that it predicts relations between the exponents of the local elastic and friction laws α_{el} and α_{visc}, and those of the macroscopic rheological response, and in good agreement with some experiments.

Finally, let us point out that the peculiar behaviour of the complex shear modulus of foams and emulsions at high frequency: $G^* \sim \sqrt{\mathrm{i}\omega}$ (Sec. II) has attracted some attention. Liu et al. [91] have proposed that it could be the signature of the presence of "weak planes" within the materials, along which bubbles (or droplets) slip with minimal mechanical stress. Alternatively, Tighe [138] have related this behaviour of G^* to the density or relaxation modes in the material.

IV. MULTISCALE FEATURES OF FOAM FLOWS

The processes at the scale of the bubbles are crucial to understand foam rheology at the macroscopic scale: as we have shown in Sec. III, the elastic modulus and the effective viscosity depend on the bubble size, and the elementary plastic event involves four bubbles. However, the connection between the sole scales of the bubble and of the foam is insufficient to understand foam rheology in several cases. First, new length scales appear as foams are confined in 2D. Then, we will show that several recent experimental results have been rationalised by the introduction of another, intermediate length scale, the cooperativity length. Finally, we will mention some specific features of strongly confined systems, when the scales of the bubble and of the full system are of the same order of magnitude.

A. Confinement effects

1. Experiments

Since foams are opaque, many experiments have focused on 2D foams to complement rheometric measurements with local measurements of velocity [30, 70, 89, 141], plasticity

[36, 43], and stresses [42]. All 2D systems resort to confining the foams with plates, with the notable exception of bubble rafts, which are dense monolayers of bubbles floating at the free surface of a soap solution.

Except some studies of complex foam flows, around obstacles [43, 44] or in constrictions [6, 42], most experiments have focussed on unidimensional Couette flows. A seminal study was performed by Debrégeas et al. [30], who studied the flow of a 2D foam, confined by a top plate, in a cylindrical Couette cell. In such a cell, the foam is placed between an inner rotating cylinder, and an outer fixed cylinder, both with cogs to prevent slip (Fig. 9). They reported an exponentially decaying velocity profile (Fig. 9), thus with a new localisation length emerging. They proposed an explanation in a stochastic model, which relates plastic flow to the stress fluctuations, as for what is commonly observed in granular systems, and reproduced localisation in simulations [68]. This study triggered a lot of interest, and different results soon appeared: Lauridsen et al. [88, 89] reported no such localisation for a bubble raft in a cylindrical Couette cell, but rather a smooth decrease followed by a jammed state, from the inner to the outer cylinder. This kind of velocity profile was also found in 3D emulsions in a cylindrical Couette cell [26], and was consistent with a Herschel–Bulkley relation. However, this viewpoint was later questioned by Katgert et al. [72], who compared the flow profiles with and without confining plates in a cylindrical Couette geometry: they showed that there was no clear hint of a jammed region close to the outer cylinder, and rationalised their results with nonlocal ingredients (see also Sec. IV B).

Other experiments have focussed on plane Couette geometries, where the foam is between two parallel plates moving at opposite velocities. In this geometry, the stress is constant across the foam, contrary to the cylindrical Couette geometry. It is actually in a plane Couette geometry that Wang et al. [141], who studied the flow with and without confining plate, showed that localisation appeared only in the presence of a confining plate, whereas the flow profile remained essentially linear in the absence of confinement (Fig. 10). Katgert et al. [70, 71] confirmed that the flow profile is localised in the presence of a confining top plate, with a localisation length decreasing at increasing velocity and liquid fraction. They also reported an effect of the foam polydispersity, which remains hitherto unexplained.

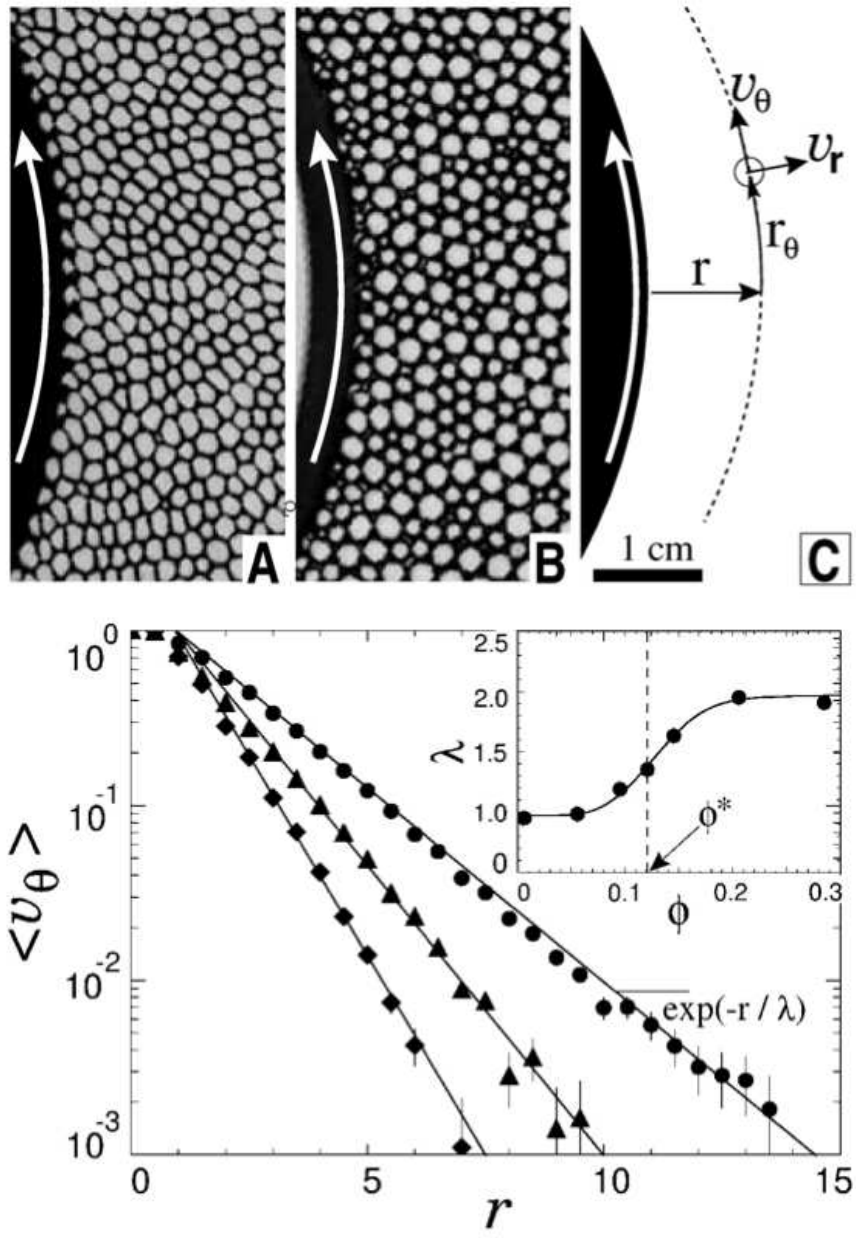

FIG. 9. Cylindrical Couette geometry from Debrégeas et al. [30] (top). The velocity field exhibits a exponential decay (bottom), with a decay length increasing with the liquid fraction (here, ϕ).

2. Models

Several models aimed at rationalising the effect of confining plates and the appearance of shear bands. Janiaud et al. [64] considered simple shear flows like the plane Couette configuration, and studied a force balance including shear elastic stress, a viscous stress proportional to the shear rate, and an external friction force proportional to the velocity.

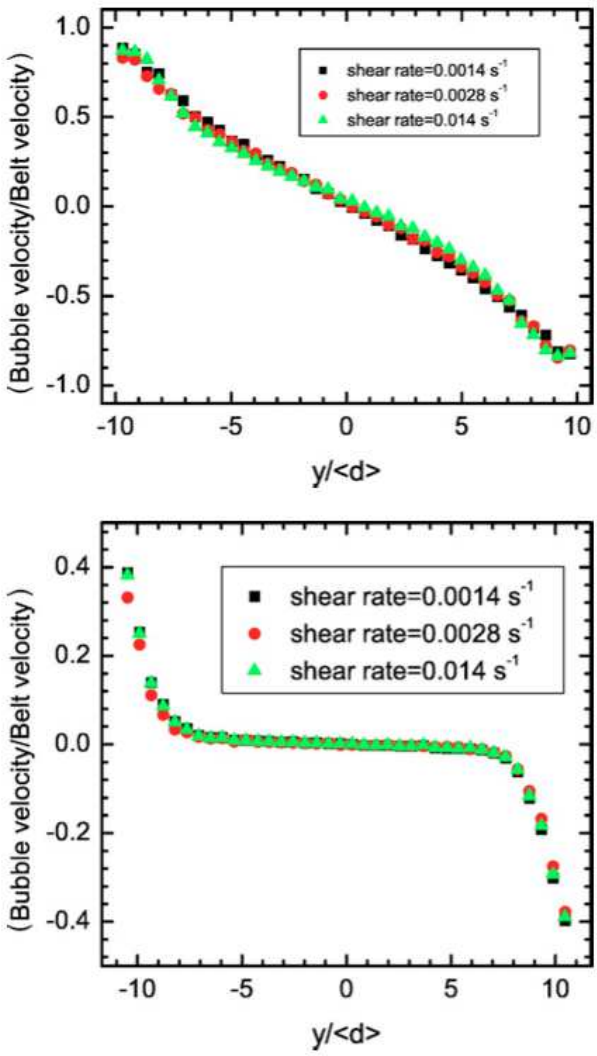

FIG. 10. Plane Couette geometry from Wang et al. [141]: velocity as a function of the spanwise coordinate y (with origin at the centre of the channel). The velocity is rescaled by that of the side belts, and y by the bubble diameter d. Velocity field without (top) and with (bottom) an upper glass plate.

This model was successful in explaining the existence of a localised profile in the presence of friction, and a linear velocity profile in its absence. Clancy et al. [21] studied the same model in cylindrical Couette geometry, and Weaire et al. [143, 144] proposed generalisations to nonlinear laws for friction and viscous stress. Katgert et al. [70, 71] used the nonlinear version of this model, with exponents deduced from rheometric measurements, to interpret the velocity profiles in their experiments. In a different spirit, Cheddadi et al. [17, 19] used a fully tensorial viscoelastoplastic model, which was successful in reproducing flows in complex

geometries like around an obstacle Cheddadi et al. [18]. In Couette geometries, they also reproduced the appearance of localisation and discussed transient effects [17], and suggested that normal stress differences could play a major role of the flow profiles [19].

B. Cooperativity/nonlocal effects

1. *Effect of a plastic event in the surrounding foam*

The importance of plastic events in foam and emulsion rheology has long been recognised. First, a T1 may be viewed as a local increment of plastic deformation, the plastic flow of foams then resulting from the superposition of many T1s, such that the local rate of strain is proportional to the rate of plastic events. Moreover, as a topological rearrangement occurs, the neighbour swapping of four bubbles (Fig. 6c–e) acts as a quadrupole of force [110] or of displacement [20] (Fig. 11a) on the surroundings; this has nonlocal effects in the surrounding foam, entraining other bubbles to be displaced and redistributing the elastic stress around, or even triggering avalanches of T1 events.

It is not yet clear how this nonlocal effect is mediated. Picard et al. [110] proposed that the medium reacts as an elastic continuum to the quadrupole of force, with an algebraically decaying influence. On the other hand, using Surface Evolver simulations, Cox et al. [28] have reported an exponentially decaying influence, with a characteristic range of a few bubble size only. Moreover, some authors have recently mentioned extremely long-range effects, reminiscent of chain forces as in granular media, either in Surface Evolver simulations (Fig. 11b) [51], or in experiments on 2D emulsions [40]. Overall, the important point is that an individual T1 has an effect over a typical size ξ significantly larger than the bubble size.

2. *Macroscopic consequences: nonlocal rheology*

Recent studies on the flow of emulsions in a straight channel of rectangular cross-section [59, 60] have called the Herschel–Bulkley law found in rheometry into question. This geometry is particularly interesting, because it enforces a linear variation across the channel of the shear stress, which vanishes at the centre and reaches its maximum at the side walls. Together with an evaluation of the shear rate from the measured velocity profile, it gives access to the relation $\sigma(\dot{\gamma})$ at the local scale. In particular, Goyon et al. [59, 60] have measured this

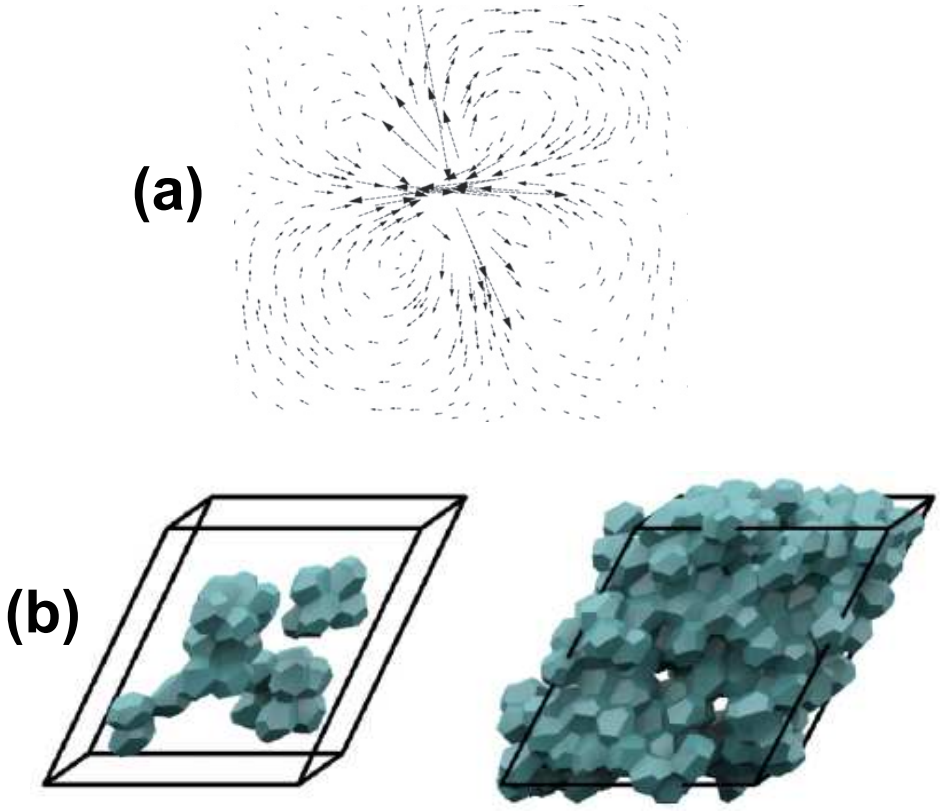

FIG. 11. (a) Quadrupolar displacement field induced by a single T1. From Surface Evolver simulations of Cox et al. [28]. (b) From Evans et al. [51]. A typical plastic zone, composed of all cells that change topology during T1 avalanche, during a Couette simulation. The stress release domain during the same T1 avalanche.

relation in a series of experiments on emulsions, and they have shown that it did not collapse on a single Herschel–Bulkley law. More precisely, the deviation from the Herschel–Bulkley flow curve obtained from macroscopic rheometry gets stronger as the driving pressure drop and the channel width decrease (Fig. 12, top).

Actually, the Herschel–Bulkley relation is a purely local relation between the shear stress and the shear rate, hence it overlooks both the elastic contribution to the stress, and the aforementioned nonlocal influence of plastic events. This is at the basis of the fluidity model, based on a kinetic theory approach [9]. It predicts that the fluidity, defined as $f = \dot{\gamma}/\tau$, is proportional to the rate of plastic events, and follows a diffusion equation:

$$f = f_{\text{bulk}} + \xi^2 \Delta f,$$

when it deviates from its bulk value, defined as $f_{\text{bulk}} = \dot{\gamma}/\tau_{\text{bulk}}$, where τ_{bulk} is given by

the Herschel–Bulkley law (1). The diffusive term quantifies in a simple way the nonlocal influence of plastic events on their surroundings. Goyon et al. [59, 60] showed that such a model was capable to reproduce well their experimental observations. The range of influence ξ appearing in this equation, called the *spatial cooperativity*, was shown to be of the order of a few times (typically, five) the droplet size. Moreover, the spatial cooperativity was shown to appear only above the jamming transition, and to be an increasing function of the packing fraction (Fig. 12, bottom).

Katgert et al. [72] studied a bubble raft under shear in a cylindrical Couette geometry, with a gap between the two cylinders equal to approximately twenty bubble radii. Like Goyon et al. [59, 60], they showed that local and global rheology did not match. In particular, they observed flow in region where the shear stress is below the rheometrically determined global yield stress. They were able to convincingly rationalise their data with the fluidity model, and obtained the cooperativity length as a fitting parameter: $\xi/\langle d\rangle = 3$ with d the bubble diameter. They claimed that ξ encodes the spatial extent of plastic rearrangements. Hence, the fluidity model provides a convenient framework to rationalise the confined flow of complex fluids.

However, at least two points remain unclear and deserve further investigation. The first is the boundary condition at solid walls, and the role of roughness. As a matter of fact, the slip velocity was let as a free fitting parameter, which certainly improves the agreement between the measurements and the predictions from the fluidity model, but does not provide any insight on the role of the walls. Only recently, Mansard et al. [94] explored the role surface boundary conditions for the flow of a dense emulsion. They show that both slippage and wall fluidisation depend non-monotonously on the roughness, a behaviour that has been interpreted with a simple model invoking the building of a stratified layer and the activation of plastic events by the surface roughness. Second, the fluidity parameter f has not been yet convincingly related to an independent measure of the local density of plastic events. In experiments, only indirect indications of such a relation have been proposed, based on the correlations of the fluctuations of the shear rate [66]. Using numerical simulations based on the bubble model [48], Mansard et al. [95] were able to measure independently the fluidity and the density of plastic events, but they show that the two quantities are not proportional; more precisely, the rearrangement rate was found to be a sublinear power (with an exponent 0.4) of the fluidity.

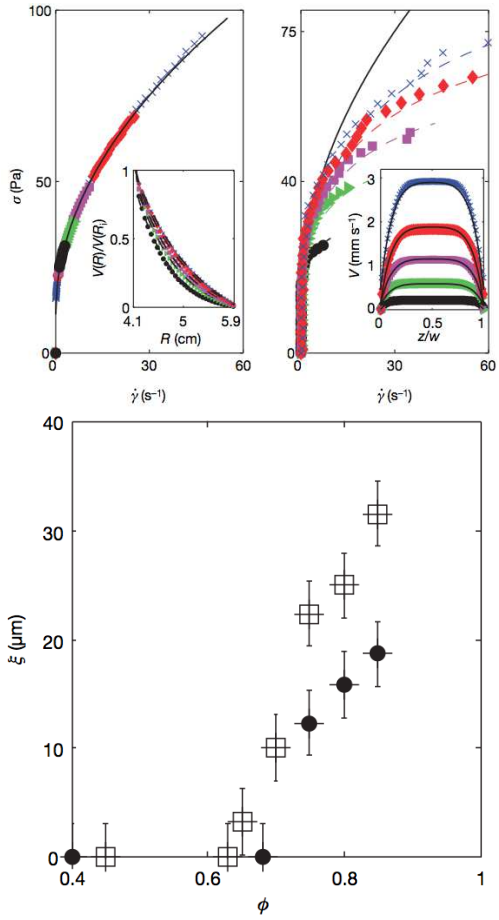

FIG. 12. Non local rheological law Goyon et al. [59]. Top left: shear stress as a function of the shear rate in Couette rheometer of wide gap (1.8 cm). The different colours stand for different rotation rates. All the data collapse on a single master curve, described by a Herschel–Bulkley relation. Inset: corresponding velocity profiles across the rheometer. Top right: shear stress as function of the shear rate across a narrow channel (width 0.25 mm), the shear rate being deduced from the measured velocity profiles across the channel (inset). The different colours stand for different pressure drops. The stress-shear rate relations do not collapse anymore onto a single curve. Bottom: cooperativity length, extracted from a fit of the velocity profiles with the fluidity model, as a function of the packing fraction $\phi = 1 - \phi_\ell$.

V. LARGE SHEAR RATES AND FREQUENCIES

A. Beyond the quasistatic limit

As long as the shear rate remains much lower than the duration t_d of the relaxation after a T1 (Sec. III B), foam rheology is quasistatic is the sense that the structure remains most of the time at equilibrium, the Plateau rules being satisfied. The rheology of foam when departing from this quasistatic limit has been studied experimentally first by Gopal and Durian [57], coupling rheometric measurements in a Couette cell with diffusive wave spectroscopy. They have showed the existence of three regimes: as very low shear rate, a regime dominated by coarsening-induced rearrangements, which has been later studied in details by Cohen-Addad et al. [22]; at intermediate shear rate, a regime dominated by shear-induced rearrangements; and at large shear rate, a regime compatible with a laminar flow of the foam, compatible with a smooth, continuous motion of the bubbles. The latter transition was found to take place a shear rate of order γ_c/t_d, with γ_c the yield strain. Interestingly, $t_d \approx 0.1$ s was also found to set the transition where the dynamic contribution of the stress overcomes the yield stress in the Herschel–Bulkley law (1): $\tau/\tau_y = 1 + (t_d\dot{\gamma})^n$ in good approximation; but this simple picture breaks down at even larger shear rates. Later Rouyer et al. [123] studied the onset of yielding in a shear startup experiment, i.e. the imposed strain γ_y at which a significant rate of rearrangements begin to occur, which is the signature of the solid-like to a liquid-like behaviour. They found a strong dependence of this strain on the shear rate, of the form $\gamma_y = \gamma_c + t'_d\dot{\gamma}$, with $\gamma_c = 0.05$ and $t'_d = 1$ s. Once again, this behaviour was ascribed to the relaxation after a T1. Recently, Marmottant and Graner [96] have proposed a simple toy model to reproduce this kind of behaviour, and its effect on the stress vs. shear rate curve.

However, in these 3D experimental studies, there is no direct link between the shear rate at which a change of flow behaviour is observed, and the local relaxation towards equilibrium of the structure after a T1. In order to access locally to the effect of the relaxation and the structure of the foam at high shear rate, 2D experiments, simulations and calculations have been proposed. In 2D experiments and in some simulations like the viscous froth model [74], the dissipation is dominated by the friction between the foam at confining walls (Sec. III C 2) instead of the viscous stress, and it is the velocity, rather than the shear rate, that controls

the departure from the quasistatic limit. At finite velocity, distorted shapes of bubbles or films are observed in experiments (Fig. 13a,b) [42, 45] and simulations [29, 49], with effects to delay the onset of T1s [49] and to modify the elastic stress [42]. If the resulting foam–wall friction overcomes surface tension, the foam even ruptures [1, 2, 4]. In some other simulations [14] and calculations [61, 79], the effect of shear rate is accounted for by a modification of the surface tension of the films, proportional to their extension rate, and the departure from quasistaticity comes from an imbalance in surface concentration. There also, the elastic stress is shown to be an increasing function of the shear rate, associated to bubble shape distortion and to delayed T1s (Fig. 13c). Hence, the increase of shear stress with shear rate contains two contributions: a viscous stress, coming from the dissipation processes within the foam structure, and also an increase of the elastic stress beyond its quasistatic value. These two contributions may be intertwined, especially if the surface tension entering the elastic stress is modified by interfacial compression or dilatation [14].

B. High frequency: waves in foams

Oscillatory rheometry is usually limited to 100 Hz. The domain of higher frequencies has been seldom explored, either to extended rheometry at higher frequencies, or to study acoustics in foams. Recently, Wintzenrieth et al. [146] exerted shear waves inside a Gillette foam using a vibrating blade. Using diffusive wave spectroscopy, they were able to extract the complex shear modulus, and they showed that the relationship $G^* \sim \sqrt{\mathrm{i}\omega}$ holds up to 1.3 kHz. Erpelding et al. [50] insonified a Gillette foam placed in a cuvette for frequencies between 0.4 and 10 kHz, and showed, also by diffusive wave spectroscopy, that the acoustically-forced foam is sheared in a thin layer close to the cuvette boundaries; they also used the relation $G^* \sim \sqrt{\mathrm{i}\omega}$ to interpret their results. Hence, this relationship seems quite robust towards high frequencies.

Acoustic forcing is another way to probe foam rheology in a less conventional way that foam rheometry, but it is complementary, because of the higher range of frequency and because it is sensitive to compressibility, which is usually neglected in rheology. Most of the existing experimental studies reported speeds of sound of order $c = 50$ m/s [54, 55, 106], close to the so-called Wood model [147]. The latter applies in the limit where the bubble size is much smaller than the acoustic wavelength, and treats foams as an effective medium, which

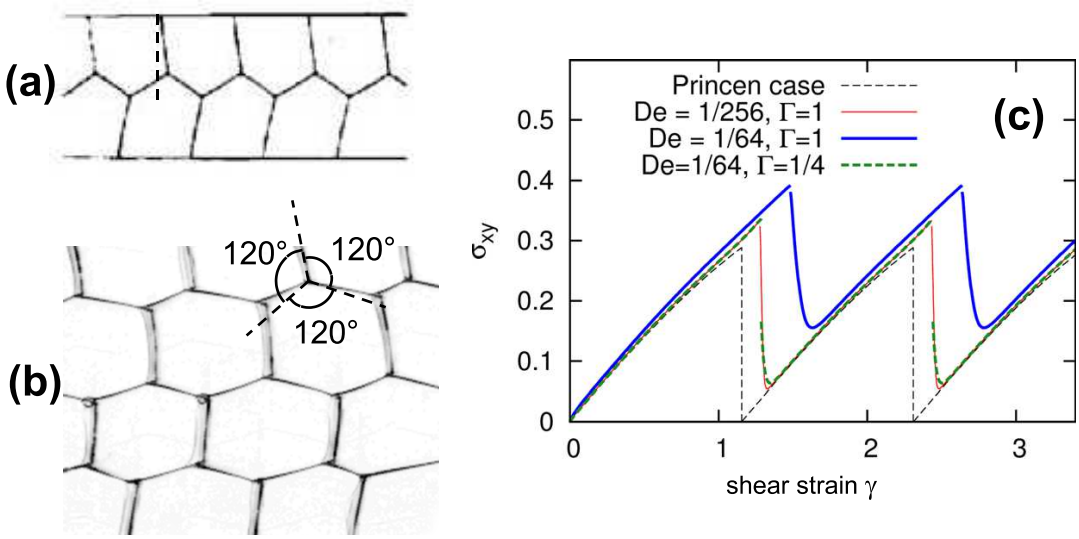

FIG. 13. (a) Staircase foam (solution of dish-washing Fairy liquid at 0.4% concentration) flowing from left to right in a microchannel (width 7 mm, depth 0.5 mm, velocity 1.5 cm/s) [45]. The films do not meet the side walls at right angles. (b) Hexagonal foam (SLES/CAPB/MAc mixture with 0.4% weight of MAc, see Golemanov et al. [56]) in a wide channel of depth 2 mm flowing from left to right and bubble area 15 mm^2. The films do not meet at 120°, and the hexagons are distorted. (c) Shear stress as a function of imposed shear strain on a Princen-like model, with a surface tension varying with the length of the films, and relaxing towards equilibrium with a relaxation time [61]. The Deborah number De is the product of the shear rate and of the relaxation time of the surfactant. As De increases, the T1s are delayed, and the average shear stress increases.

density ρ_{eff} and compressibility χ_{eff} are given by the mixture law, *i.e.* averages of those of the gas and liquid phases, weighted by their respective volume fractions: $c = (\rho_{\text{eff}}\chi_{\text{eff}})^{-1/2}$. However, much higher speeds of sound, of order 200 m/s, were also measured [105]. Another model was then proposed by Kann [69], who considered the foam as an assembly of thin soap films (of thickness h) surrounded by air, and derived: $c = c_g/(1+\rho_\ell h/\rho_g a)$, with c_g the speed of sound in the gas, ρ_ℓ the density of liquid and ρ_g that of gas. Moreover, some studies reported a resonant behaviour [5, 41]. Recently, these seemingly contradictory results were explained in a unified framework by Pierre et al. [111]. They showed experimentally and theoretically that Wood's model is the limit of low frequencies and small bubbles, Kann's model is the limit of high frequencies and large bubbles, and that there is a resonance in between, with a maximum of attenuation. This was explained by considering that the

liquid contained within the foam is distributed either in thin soap films, or in much thicker Plateau borders and vertices. In particular, while all these elements vibrate in phase with the pressure wave at low frequency (and small bubble size), which is the implicit assumption justifying the use of an average density in Wood's model, the inertia of the Plateau borders and vertices is such that their vibration amplitude becomes negligible with respect to that of the films at high frequency (and large bubble size), justifying Kann's model in this limit. The dissipative properties of foams, discussed in Sec. III C, are also used to mitigate the huge pressure waves associated to shocks, blasts and explosions [12, 31, 117], although it is still unclear which is the dominant dissipative mechanism at stake in such extreme conditions.

VI. CONCLUSIONS

The local mechanisms dominating dissipation in foams still remain elusive. Notably, more research is needed to understand the precise links between surfactant dynamics (namely, their surface elasticity and their exchanges between interfaces and bulk) and macroscopic measurements of dissipation, such as the loss modulus.

There is still a lack of data at the local scale in the bulk of a 3D foam. Time and space-resolved measurements of the deformations, elastic stresses, and distribution of plastic events still remains an experimental challenge. The progress of fast X-ray tomography [93, 104] and confocal microscopy (at least for index-matched emulsions) [66, 67] brings some hope that this challenge will be overcome in the near future.

Finally, if most of the research focuses on interpreting rheometry measurements at the scale of the foam with considerations at the microstructure scale, little is known about the effect of the flow on the microstructure and its potential feedback. Regarding emulsions, this question was already raised by Taylor [136] in the context of the formation of emulsions. Droplets can either break [39] or coalesce [10] due to the interaction with the flow. Such coupling might be very relevant for foams deformed at high shear rates.

ACKNOWLEDGMENTS

We acknowledge funding support from the GDR 2983 Mousses (CNRS) for supporting travel expenses.

---

[1] S. Arif, J. C. Tsai, and S. Hilgenfeldt. Speed of crack propagation in dry aqueous foams. *EPL*, 92:38001, 2010.

[2] S. Arif, J. C. Tsai, and S. Hilgenfeldt. Spontaneous brittle-to-ductile transition in aqueous foam. *J. Rheol.*, 56:485–499, 2012.

[3] G. K. Batchelor. The stress system in a suspension of force-free particules. *J. Fluid Mech.*, 41:545–570, 1970.

[4] I. Ben Salem, I. Cantat, and B. Dollet. Response of a two-dimensional liquid foam to air injection: swelling rate, fingering and fracture. *J. Fluid Mech.*, 714:258–282, 2013.

[5] I. Ben Salem, R. M. Guillermic, C. Sample, V. Leroy, A. Saint-Jalmes, and B. Dollet. Propagation of ultrasound in aqueous foams: bubble size dependence and resonance effects. *Soft Matter*, 9:1194–1202, 2013.

[6] Y. Bertho, C. Becco, and N. Vandewalle. Dense bubble flow in a silo: an unusual flow of a dispersed medium. *Phys. Rev. E*, 73:056309, 2006.

[7] A. L. Biance, S. Cohen-Addad, and R. Höhler. Topological transition dynamics in a strained bubble cluster. *Soft Matter*, 5:4672–4679, 2009.

[8] A. L. Biance, A. Delbos, and O. Pitois. How topological rearrangements and liquid fraction control liquid foam stability. *Phys. Rev. Lett.*, 106:068301, 2011.

[9] L. Bocquet, A. Colin, and A. Ajdari. Kinetic theory of plastic flow in soft glassy materials. *Phys. Rev. Lett.*, 103:036001, 2009.

[10] N. Bremond, H. Doméjean, and J. Bibette. Propagation of drop coalescence in a two-dimensional emulsion: a route towards phase inversion. *Phys. Rev. Lett.*, 106:214502, 2011.

[11] F. P. Bretherton. The motion of long bubbles in tubes. *J. Fluid Mech.*, 10:166–188, 1961.

[12] A. Britan, M. Liverts, and G. Ben-Dor. Mitigation of sound waves by wet aqueous foams. *Colloids Surf. A*, 344:48–55, 2009.

[13] D. M. A. Buzza, C. Y. D. Lu, and M. E. Cates. Linear shear rheology of incompressible foams. *J. Phys. II France*, 5:37–52, 1995.

[14] I. Cantat. Gibbs elasticity effect in foam shear flows: a non quasi-static 2D numerical simulation. *Soft Matter*, 7:448–455, 2011.

[15] I. Cantat. Liquid meniscus friction on a wet plate: Bubbles, lamellae, and foams. *Phys. Fluids*, 25:031303, 2013.

[16] I. Cantat, S. Cohen-Addad, F. Elias, F. Graner, R. Höhler, O. Pitois, F. Rouyer, and A. Saint-Jalmes. *Foams*. Oxford University Press, 2013.

[17] I. Cheddadi, P. Saramito, C. Raufaste, P. Marmottant, and F. Graner. Numerical modelling of foam couette flows. *Eur. Phys. J. E*, 27:123–133, 2008.

[18] I. Cheddadi, P. Saramito, B. Dollet, C. Raufaste, and F. Graner. Understanding and predicting viscous, elastic, plastic flows. *Eur. Phys. J. E*, 34:1, 2011.

[19] I. Cheddadi, P. Saramito, and F. Graner. Steady couette flows of elastoviscoplastic fluids are non-unique. *J. Rheol.*, 56:213–239, 2012.

[20] D. Chen, K. W. Desmond, and E. R. Weeks. Topological rearrangements and stress fluctuations in quasi-two-dimensional hopper flow of emulsions. *Soft Matter*, 8:10486–10492, 2012.

[21] R. J. Clancy, E. Janiaud, D. Weaire, and S. Hutzler. The response of 2D foams to continuous applied shear in a Couette rheometer. *Eur. Phys. J. E*, 21:123–132, 2006.

[22] S. Cohen-Addad, R. Höhler, and Y. Khidas. Origin of the slow linear viscoelastic response of aqueous foams. *Phys. Rev. Lett.*, 93:028302, 2004.

[23] S. Cohen-Addad, R. Höhler, and O. Pitois. Flow in foams and flowing foams. *Annu. Rev. Fluid Mech.*, 45:241–267, 2013.

[24] S. Courty, B. Dollet, F. Elias, P. Heinig, and F. Graner. Two-dimensional shear modulus of a Langmuir foam. *Europhys. Lett.*, 64:709–715, 2003.

[25] P. Coussot. *Rheometry of Pastes, Suspensions and Granular Materials*. Wiley, 2005.

[26] P. Coussot, J. S. Raynaud, F. Bertrand, P. Moucheront, J. P. Guilbaud, H. T. Huynh, S. Jarny, and D. Lesueur. Coexistence of liquid and solid phases in flowing soft-glassy materials. *Phys. Rev. Lett.*, 88:218301, 2002.

[27] S. J. Cox and E. L. Whittick. Shear modulus of two-dimensional foams: The effect of area dispersity and disorder. *Eur. Phys. J. E*, 21:49–56, 2006.

[28] S. J. Cox, F. Graner, and M. F. Vaz. Screening in dry two-dimensional foams. *Soft Matter*, 4:1871–1878, 2008.

[29] S. J. Cox, D. Weaire, and G. Mishuris. The viscous froth model: steady states and the high-velocity limit. *Proc. Roy. Soc. A*, 465:2391–2405, 2010.

[30] G. Debrégeas, H. Tabuteau, and J.-M. di Meglio. Deformation and flow of a two-dimensional foam under continuous shear. *Phys. Rev. Lett.*, 87:178305, 2001.

[31] E. Del Prete, A. Chinnayya, L. Domergue, A. Hadjadj, and J. F. Haas. Blast wave mitigation by dry aqueous foams. *Shock Waves*, 23:39–53, 2013.

[32] N. D. Denkov, V. Subramanian, D. Gurovich, and A. Lips. Wall slip and viscous dissipation in sheared foams: Effect of surface mobility. *Colloids Surf. A*, 263:129–145, 2005.

[33] N. D. Denkov, S. Tcholakova, K. Golemanov, V. Subramanian, and A. Lips. Foam-wall friction: Effect of air volume fraction for tangentially immobile bubble surface. *Colloids Surf. A*, 282:329–347, 2006.

[34] N. D. Denkov, S. Tcholakova, K. Golemanov, K. P. Ananthapadmanabhan, and A. Lips. Viscous friction in foams and concentrated emulsions under steady shear. *Phys. Rev. Lett.*, 100:138301, 2008.

[35] N. D. Denkov, S. Tcholakova, K. Golemanov, K. P. Ananthapadmanabhan, and A. Lips. The role of surfactant type and bubble surface mobility in foam rheology. *Soft Matter*, 5: 3389–3408, 2009.

[36] M. Dennin. Statistics of bubble rearrangements in a slowly sheared two-dimensional foam. *Phys. Rev. E*, 70:041406, 2004.

[37] M. Dennin and C. M. Knobler. Experimental studies of bubble dynamics in a slowly driven monolayer foam. *Phys. Rev. Lett.*, 78:2485–2488, 1997.

[38] B. Derjaguin. Die elastischen Eigenschaften der Schäume. *Kolloid Z.*, 64:1–6, 1933.

[39] S. R. Derkach. Rheology of emulsions. *Adv. Colloid Interface Sci.*, 151:1–23, 2009.

[40] K. W. Desmond, P. J. Young, D. Chen, and E. R. Weeks. Experimental study of forces between quasi-two-dimensional emulsion droplets near jamming. *Soft Matter*, 9:3424–3436, 2013.

[41] J. Ding, F. W. Tsaur, A. Lips, and A. Akay. Acoustical observation of bubble oscillations induced by bubble popping. *Phys. Rev. E*, 75:041601, 2007.

[42] B. Dollet. Local description of the two-dimensional flow of foam through a contraction. *J. Rheol.*, 54:741–760, 2010.

[43] B. Dollet and F. Graner. Two-dimensional flow of foam around a circular obstacle: local measurements of elasticity, plasticity and flow. *J. Fluid Mech.*, 585:181–211, 2007.

[44] B. Dollet, M. Aubouy, and F. Graner. Anti-inertial lift in foams: A signature of the elasticity of complex fluids. *Phys. Rev. Lett.*, 95:168303, 2005.

[45] W. Drenckhan, S. J. Cox, G. Delaney, H. Holste, D. Weaire, and N. Kern. Rheology of ordered foams—on the way to discrete microfluidics. *Colloids Surf. A*, 263:52–64, 2005.

[46] M. Durand and H. A. Stone. Relaxation time of the topological T1 process in a two-dimensional foam. *Phys. Rev. Lett.*, 97:226101, 2006.

[47] M. Durand, J. Käfer, C. Quilliet, S. Cox, S. Ataei Talebi, and F. Graner. Statistical mechanics of two-dimensional shuffled foams: Prediction of the correlation between geometry and topology. *Phys. Rev. Lett.*, 107:168304, 2011.

[48] D. J. Durian. Bubble-scale model of foam mechanics: Melting, nonlinear behavior, and avalanches. *Phys. Rev. E*, 55:1739–1751, 1997.

[49] B. Embley and P. Grassia. Viscous froth simulations with surfactant mass transfer and Marangoni effects: Deviations from Plateau's rules. *Colloids Surf. A*, 382:8–17, 2011.

[50] M. Erpelding, R. M. Guillermic, B. Dollet, A. Saint-Jalmes, and J. Crassous. Investigating acoustic-induced deformations in a foam using multiple light scattering. *Phys. Rev. E*, 82: 021409, 2010.

[51] M. E. Evans, A. M. Kraynik, D. A. Reinelt, K. Mecke, and G. E. Schröder-Turk. Networklike propagation of cell-level stress in sheared random foams. *Phys. Rev. Lett.*, 111:138301, 2013.

[52] M. L. Falk and J. S. Langer. Dynamics of viscoplastic deformation in amorphous solids. *Phys. Rev. E*, 57:7192–7205, 1998.

[53] A. S. Gittings and D. J. Durian. Statistics of bubble rearrangement dynamics in a coarsening foam. *Phys. Rev. E*, 78:066303, 2008.

[54] I. Goldfarb, Z. Orenbakh, I. Shreiber, and F. Vafina. Sound and weak shock wave propagation in gas-liquid foams. *Shock Waves*, 7:77–88, 1997.

[55] I. I. Goldfarb, I. R. Shreiber, and F. I. Vafina. Heat transfer effect on sound propagation in foam. *J. Acoust. Soc. Am.*, 92:2756–2769, 1992.

[56] K. Golemanov, N. D. Denkov, S. Tcholakova, M. Vethamuthu, and A. Lips. Surfactant mixtures for control of bubble surface mobility in foam studies. *Langmuir*, 24:9956–9961, 2008.

[57] A. D. Gopal and D. J. Durian. Shear-induced "melting" of an aqueous foam. *J. Colloid Interface Sci.*, 213:169–178, 1999.

[58] A. D. Gopal and D. J. Durian. Relaxing in foam. *Phys. Rev. Lett.*, 91:188303, 2003.

[59] J. Goyon, A. Colin, G. Ovarlez, A. Ajdari, and L. Bocquet. Spatial cooperativity in soft glassy flows. *Nature*, 454:84–87, 2008.

[60] J. Goyon, A. Colin, and L. Bocquet. How does a soft glassy material flow: finite size effects, non local rheology, and flow cooperativity. *Soft Matter*, 6:2668–2678, 2010.

[61] P. Grassia, B. Embley, and C. Oguey. A Princen hexagonal foam out of physicochemical equilibrium. *J. Rheol.*, 56:501–526, 2012.

[62] R. Höhler and S. Cohen-Addad. Rheology of liquid foams. *J. Phys. Condens. Matter*, 17: R1041–R1069, 2005.

[63] J. N. Israelachvili. *Intermolecular and Surface Forces*. Academic Press, 1991. 2nd Edition.

[64] É. Janiaud, D. Weaire, and S. Hutzler. Two-dimensional foam rheology with viscous drag. *Phys. Rev. Lett.*, 97:038302, 2006.

[65] S. A. Jones, B. Dollet, Y. Méheust, S. J. Cox, and I. Cantat. Structure-dependent mobility of a dry aqueous foam flowing along two parallel channels. *Phys. Fluids*, 25:063101, 2013.

[66] P. Jop, V. Mansard, P. Chaudhuri, L. Bocquet, and A. Colin. Microscale rheology of a soft glassy material close to yielding. *Phys. Rev. Lett.*, 108:148301, 2012.

[67] I. Jorjadze, L. L. Pontani, and J. Brujić. Microscopic approach to the nonlinear elasticity of compressed emulsions. *Phys. Rev. Lett.*, 110:048302, 2013.

[68] A. Kabla and G. Debrégeas. Local stress relaxation and shear banding in a dry foam under shear. *Phys. Rev. Lett.*, 90:258303, 2003.

[69] K. B. Kann. Sound waves in foams. *Colloids Surf. A*, 263:315–319, 2005.

[70] G. Katgert, M. E. Möbius, and M. van Hecke. Rate dependence and role of disorder in linearly sheared two-dimensional foams. *Phys. Rev. Lett.*, 101:058301, 2008.

[71] G. Katgert, A. Latka, M. E. Möbius, and M. van Hecke. Flow in linearly sheared two-dimensional foams: From bubble to bulk scale. *Phys. Rev. E*, 79:066318, 2009.

[72] G. Katgert, B. P. Tighe, M. E. Mbius, and M. van Hecke. Couette flow of two-dimensional foams. *EPL*, 90:54002, 2010.

[73] G. Katgert, B. P. Tighe, and M. van Hecke. The jamming perspective on wet foams. *Soft Matter*, 9:9739–9743, 2013.

[74] N. Kern, D. Weaire, A. Martin, S. Hutzler, and S. J. Cox. Two-dimensional viscous froth model for foam dynamics. *Phys. Rev. E*, 70:041411, 2004.

[75] S. A. Khan and R. C. Armstrong. Rheology of foams I. Theory for dry foams. *J. Non-Newtonian Fluid Mech.*, 22:1–22, 1986.

[76] S. A. Khan and R. C. Armstrong. Rheology of foams IV. Effect of gas volume fraction. *J. Rheol.*, 33:881–911, 1989.

[77] S. A. Koehler, S. Hilgenfeldt, and H. A. Stone. Liquid flow through aqueous foams: The node-dominated foam drainage equation. *Phys. Rev. Lett.*, 82:4232–4235, 1999.

[78] A. M. Kraynik. Foam flows. *Annu. Rev. Fluid Mech.*, 20:325–357, 1988.

[79] A. M. Kraynik and M. G. Hansen. Foam rheology: A model of viscous phenomena. *J. Rheol.*, 31:175–205, 1987.

[80] A. M. Kraynik and D. A. Reinelt. Linear elastic behavior of dry soap foams. *J. Colloid Interface Sci.*, 181:511–520, 1996.

[81] A. M. Kraynik, D. A. Reinelt, and F. van Swol. Structure of random foams. *Phys. Rev. Lett.*, 93:208301, 2004.

[82] K. Krishan, A. Helal, R. Höhler, and S. Cohen-Addad. Fast relaxations in foam. *Phys. Rev. E*, 82:011405, 2010.

[83] N. P. Kruyt. On the shear modulus of two-dimensional liquid foams: A theoretical study of the effect of geometrical disorder. *J. Appl. Mech.*, 74:560–567, 2007.

[84] M.-D. Lacasse, G. S. Grest, D. Levine, T. G. Mason, and D. A. Weitz. Model for the elasticity of compressed emulsions. *Phys. Rev. Lett.*, 76:3448, 1996.

[85] J. Lambert, I. Cantat, R. Delannay, R. Mokso, P. Cloetens, J. A. Glazier, and F. Graner. Coarsening foams robustly reach a self-similar growth regime. *Phys. Rev. Lett.*, 104:248304, 2010.

[86] D. Langevin. Rheology of adsorbed surfactant monolayers at fluid surfaces. *Annu. Rev. Fluid Mech.*, 46:47–65, 2014.

[87] R. G. Larson. *The Structure and Rheology of Complex Fluids.* Oxford University Press, 1999.

[88] J. Lauridsen, M. Twardos, and M. Dennin. Shear-induced stress relaxation in a two-dimensional wet foam. *Phys. Rev. Lett.*, 89:098303, 2002.

[89] J. Lauridsen, G. Chanan, and M. Dennin. Velocity profiles in slowly sheared bubbles rafts. *Phys. Rev. Lett.*, 93:018303, 2004.

[90] M. Le Merrer, S. Cohen-Addad, and R. Höhler. Bubble rearrangement duration in foams near the jamming point. *Phys. Rev. Lett.*, 108:188301, 2012.

[91] A. J. Liu, S. Ramaswamy, T. G. Mason, H. Gang, and D. A. Weitz. Anomalous viscous loss in emulsions. *Phys. Rev. Lett.*, 76:3017–3020, 1996.

[92] C. W. Macosko. *Rheology: Principles, Measurements and Applications*. Wiley–VCH, 1994.

[93] K. Mader, R. Mokso, C. Raufaste, B. Dollet, S. Santucci, J. Lambert, and M. Stampanoni. Quantitative 3D characterization of cellular materials: Segmentation and morphology of foam. *Colloids Surf. A*, 415:230–238, 2012.

[94] V. Mansard, L. Bocquet, and A. Colin. Boundary conditions for soft glassy flows: slippage and surface fluidization. *Soft Matter*. to appear.

[95] V. Mansard, A. Colin, P. Chaudhuri, and L. Bocquet. A molecular dynamics study of non-local effects in the flow of soft jammed particles. *Soft Matter*, 9:7489–7500, 2013.

[96] P. Marmottant and F. Graner. Plastic and viscous dissipations in foams: cross-over from low to high shear rates. *Soft Matter*, 9:9602–9607, 2013.

[97] P. Marmottant and J. P. Raven. Microfluidics with foams. *Soft Matter*, 5:3385–3388, 2009.

[98] S. Marze, D. Langevin, and A. Saint-Jalmes. Aqueous foam slip and shear regimes determined by rheometry and multiple light scattering. *J. Rheol.*, 52:1091–1111, 2008.

[99] S. Marze, R. M. Guillermic, and A. Saint-Jalmes. Oscillatory rheology of aqueous foams: surfactant, liquid fraction, experimental protocol and aging effects. *Soft Matter*, 5:1937–1946, 2009.

[100] T. G. Mason, J. Bibette, and D. A. Weitz. Elasticity of compressed emulsions. *Phys. Rev. Lett.*, 75:2051–2054, 1995.

[101] T. G. Mason, J. Bibette, and D. A. Weitz. Yielding and flow of monodisperse emulsions. *J. Colloid Interface Sci.*, 179:439–448, 1996.

[102] T. G. Mason, M. D. Lacasse, G. S. Grest, D. Levine, J. Bibette, and D. A. Weitz. Osmotic pressure and viscoelastic shear moduli of concentrated emulsions. *Phys. Rev. E*, 56:3150–3166, 1997.

[103] M. P. Miklius and S. Hilgenfeldt. Analytical results for size–topology correlations in 2D disk and cellular packings. *Phys. Rev. Lett.*, 108:015502, 2012.

[104] R. Mokso, F. Marone, and M. Stampanoni. Real-time tomography at the swiss light source. *AIP Conference Proceedings*, SRI2009, 2009.

[105] N. T. Moxon, A. C. Torrance, and S. B. Richardson. The attenuation of acoustic signals by aqueous and particulate foams. *Appl. Acoust.*, 24:193–209, 1988.

[106] N. Mujica and S. Fauve. Sound velocity and absorption in a coarsening foam. *Phys. Rev. E*, 66:021404, 2002.

[107] K. J. Mysels, K. Shinoda, and S. Frankel. *Soap Films: Study of Their Thinning and a Bibliography.* Pergamon, 1959.

[108] G. Ovarlez, S. Rodts, A. Ragouilliaux, P. Coussot, J. Goyon, and A. Colin. Wide-gap Couette flows of dense emulsions: Local concentration measurements, and comparison between macroscopic and local constitutive law measurements through magnetic resonance imaging. *Phys. Rev. E*, 78:036307, 2008.

[109] G. Ovarlez, K. Krishan, and S. Cohen-Addad. Investigation of shear banding in three-dimensional foams. *EPL*, 91:68005, 2010.

[110] G. Picard, A. Ajdari, F. Lequeux, and L. Bocquet. Elastic consequences of a single plastic event: A step towards the microscopic modeling of the flow of yield stress fluids. *Eur. Phys. J. E*, 15:371–381, 2004.

[111] J. Pierre, B. Dollet, and V. Leroy. Resonant acoustic propagation and negative density in liquid foams. *Phys. Rev. Lett.*, 112:148307, 2014.

[112] J. A. F. Plateau. *Statique expérimentale et théorique des liquides soumis aux seules forces moléculaires.* Gauthier–Villars, 1873.

[113] H. M. Princen. Rheology of foams and highly concentrated emulsions. I. Elastic properties and yield stress of a cylindrical model system. *J. Colloid Interface Sci.*, 91:160–175, 1983.

[114] H. M. Princen. Rheology of foams and highly concentrated emulsions. II. Experimental study of the yield stress and wall effects for concentrated oil-in-water emulsions. *J. Colloid Interface Sci.*, 105:150–171, 1985.

[115] H. M. Princen and A. D. Kiss. Rheology of foams and highly concentrated emulsions. III. Static shear modulus. *J. Colloid Interface Sci.*, 112:427–437, 1986.

[116] H. M. Princen and A. D. Kiss. Rheology of foams and highly concentrated emulsions. IV. An experimental study of the shear viscosity and yield stress of concentrated emulsions. *J. Colloid Interface Sci.*, 128:176–187, 1989.

[117] R. Raspet and S. K. Griffiths. The reduction of blast noise with aqueous foams. *J. Acoust. Soc. Am.*, 74:1757–1763, 1983.

[118] C. Raufaste, B. Dollet, S. Cox, Y. Jiang, and F. Graner. Yield drag in a two-dimensional foam flow around a circular obstacle: Effect of liquid fraction. *Eur. Phys. J. E*, 23:217–228, 2007.

[119] D. A. Reinelt and A. M. Kraynik. Viscous effects in the rheology of foams and concentrated emulsions. *J. Colloid Interface Sci.*, 132:491–503, 1989.

[120] D. A. Reinelt and A. M. Kraynik. Simple shearing flow of a dry kelvin soap foam. *J. Fluid Mech.*, 311:327–343, 1996.

[121] D. A. Reinelt and A. M. Kraynik. Simple shearing flow of dry soap foams with tetrahedrally close-packed structure. *J. Rheol.*, 44:453–471, 2000.

[122] W. R. Rossen. Theory of mobilization pressure gradient of flowing foams in porous media. I. Incompressible foam. *J. Colloid Interface Sci.*, 136:1–16, 1990.

[123] F. Rouyer, S. Cohen-Addad, M. Vignes-Adler, and R. Höhler. Dynamics of yielding observed in a three-simensional aqueous dry foam. *Phys. Rev. E*, 267:021405, 2003.

[124] F. Rouyer, S. Cohen-Addad, and R. Höhler. Is the yield stress of aqueous foam a well-defined quantity? *Colloids Surf. A*, 263:111–116, 2005.

[125] F. Rouyer, S. Cohen-Addad, R. Höhler, P. Sollich, and S. M. Fielding. The large amplitude oscillatory strain response of aqueous foam: Strain localization and full stress Fourier spectrum. *Eur. Phys. J. E*, 27:309–321, 2008.

[126] A. Saint-Jalmes and D. J. Durian. Vanishing elasticity for wet foams: Equivalence with emulsions and rol of polydispersity. *J. Rheol.*, 43:1411–1422, 1999.

[127] L. Saulnier, F. Restagno, J. Delacotte, D. Langevin, and E. Rio. What is the mechanism of soap film entrainment? *Langmuir*, 27:13406–13409, 2011.

[128] L. L. Schramm. *Foams: Fundamentals and Applications in the Petroleum Industry.* American Chemical Society, 1994.

[129] L. W. Schwartz and H. M. Princen. A theory of extensional viscosity for flowing foams and concentrated emulsions. *J. Colloid Interface Sci.*, 118:201–211, 1987.

[130] J. Seiwert, M. Monloubou, B. Dollet, and I. Cantat. Extension of a suspended soap film: a homogeneous dilatation followed by new film extraction. *Phys. Rev. Lett.*, 111:094501, 2013.

[131] J. Seiwert, B. Dollet, and I. Cantat. Theoretical study of the generation of soap films: role of interfacial visco-elasticity. *J. Fluid Mech.*, 739:124–142, 2014.

[132] P. Sollich, F. Lequeux, P. Hébraud, and M. E. Cates. Rheology of soft glassy materials. *Phys. Rev. Lett.*, 78:2020–2023, 1997.

[133] D. Stamenović. A model of foam elasticity based upon the laws of Plateau. *J. Colloid Interface Sci.*, 145:255–259, 1991.

[134] P. Stevenson, editor. *Foam Engineering: Fundamentals and Applications*. Wiley, 2012.

[135] C. Stubenrauch and R. von Klitzing. Disjoining pressure in thin liquid foam and emulsion films—new concepts and perspectives. *J. Phys. Condens. Matter*, 15:R1197–R1232, 2003.

[136] G. I. Taylor. The formation of emulsions in definable fields of flow. *Proc. R. Soc. Lond. A*, 146:501–523, 1934.

[137] S. Tcholakova, N. D. Denkov, K. Golemanov, K. P. Ananthapadmanabhan, and A. Lips. Theoretical model of viscous friction inside steadily sheared foams and concentrated emulsions. *Phys. Rev. E*, 78:011405, 2008.

[138] B. P. Tighe. Relaxations and rheology near jamming. *Phys. Rev. Lett.*, 107:158303, 2011.

[139] B. P. Tighe, E. Woldhuis, J. J. C. Remmers, W. van Saarloos, and M. van Hecke. Model for the scaling of stresses and fluctuations in flows near jamming. *Phys. Rev. Lett.*, 105:088303, 2010.

[140] M. van Hecke. Jamming of soft particles: geometry, mechanics, scaling and isostaticity. *J. Phys. Condens. Matter*, 22:033101, 2010.

[141] Y. Wang, K. Krishan, and M. Dennin. Impact of boundaries on velocity profiles in bubble rafts. *Phys. Rev. E*, 73:031401, 2006.

[142] D. Weaire and S. Hutzler. *The Physics of Foams*. Oxford University Press, 1999.

[143] D. Weaire, S. Hutzler, V. J. Langlois, and R. J. Clancy. Velocity dependence of shear localisation in a 2D foam. *Phil. Mag. Lett.*, 88:387–396, 2008.

[144] D. Weaire, R. J. Clancy, and S. Hutzler. A simple analytical theory of localisation in 2D foam rheology. *Phil. Mag. Lett.*, 89:294–299, 2009.

[145] S. J. Weinstein and K. J. Ruschak. Coating flows. *Annu. Rev. Fluid Mech.*, 36:29–53, 2004.

[146] F. Wintzenrieth, S. Cohen-Addad, M. Le Merrer, and R. Höhler. Laser-speckle-visibility acoustic spectroscopy in soft turbid media. *Phys. Rev. E*, 89:012308, 2014.

[147] A. B. Wood. *A Textbook on Sound*. Bell, 1944.

[148] M. Wyart, H. Liang, A. Kabla, and L. Mahadevan. Elasticity of floppy and stiff random networks. *Phys. Rev. Lett.*, 101:215501, 2008.